



HAL
open science

Optimal Triangular Haar Bases for Spherical Data

Georges-Pierre Bonneau

► **To cite this version:**

Georges-Pierre Bonneau. Optimal Triangular Haar Bases for Spherical Data. Visualization '99, Oct 1999, San Francisco, United States. 10.1109/VISUAL.1999.809898 . hal-01708564

HAL Id: hal-01708564

<https://inria.hal.science/hal-01708564v1>

Submitted on 14 Feb 2018

HAL is a multi-disciplinary open access archive for the deposit and dissemination of scientific research documents, whether they are published or not. The documents may come from teaching and research institutions in France or abroad, or from public or private research centers.

L'archive ouverte pluridisciplinaire **HAL**, est destinée au dépôt et à la diffusion de documents scientifiques de niveau recherche, publiés ou non, émanant des établissements d'enseignement et de recherche français ou étrangers, des laboratoires publics ou privés.

Optimal Triangular Haar Bases for Spherical Data

Georges-Pierre Bonneau*

LMC - CNRS

Abstract

Multiresolution analysis based on FWT (Fast Wavelet Transform) is now widely used in Scientific Visualization. Spherical bi-orthogonal wavelets for spherical triangular grids were introduced in [5]. In order to improve on the orthogonality of the wavelets, the concept of nearly orthogonality, and two new piecewise-constant (Haar) bases were introduced in [4]. In our paper, we extend the results of [4]. First we give two one-parameter families of triangular Haar wavelet bases that are nearly orthogonal in the sense of [4]. Then we introduce a measure of orthogonality. This measure vanishes for orthogonal bases. Eventually, we show that we can find an optimal parameter of our wavelet families, for which the measure of orthogonality is minimized. Several numerical and visual examples for a spherical topographic data set illustrates our results.

Keywords and phrases: visualization, multiresolution, wavelets, orthogonality.

1 INTRODUCTION

Representing large data sets by decomposition in a wavelet basis has many applications in scientific visualization. This includes LOD (level of detail) visualization, local area zooming, progressive transmission over networks, compression, and others ([6]). Since wavelets were originally discovered in signal analysis, where the data comes from regular samples, their application in scientific visualization began with uniformly gridded data sets. An important application domain for uniformly gridded data visualization is volume visualization ([2]).

In the last few years, a major challenge has been to extend wavelet decompositions to work on more general data sets. The introduction of triangular wavelets in [3] for geometric meshes, and triangular spherical wavelets in [5] for scalar spherical data sets, were two crucial steps in that challenge. More recently, generalized Haar wavelets for irregular triangulations have been introduced in [1].

Triangular wavelets are defined over nested triangular grids. These grids are the result of a subdivision process starting on a base triangular mesh, and dividing recursively each triangle into four sub-triangles by inserting new vertices at the midpoint of each edge. In

the case of spherical data, each edge is part of a great circle, the midpoint is the geodesic bisector, and the base mesh may be either a spherical tetrahedron, octahedron or icosahedron, see Fig. 1.

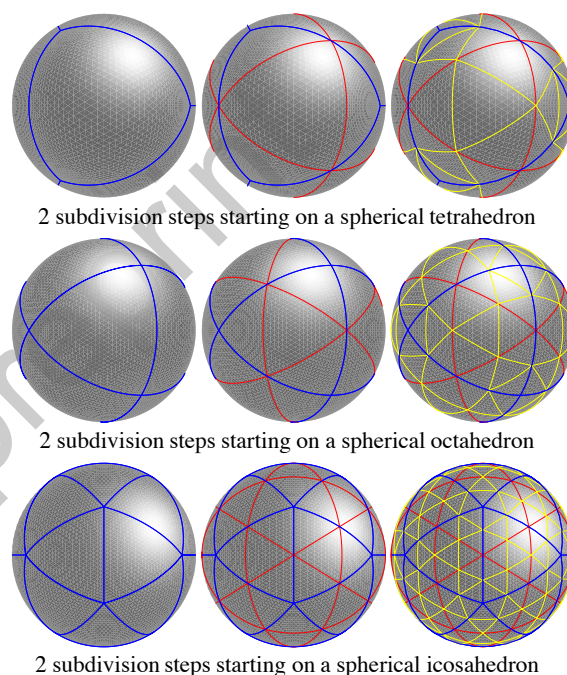


Figure 1: Subdivision of spherical triangular meshes

This paper deals with piecewise constant triangular wavelets. While this may be seen as a restriction for smooth data sets, it is sufficient for large and non-smooth data. In particular, many earth data sets, which are of special interest in scientific visualization, are usually non-smooth, and thus can be tackled efficiently with piecewise constant wavelets. This has been verified in [5] where Haar bases are shown to work as good as smoother bases for the compression of the topographic data set that we will use in our illustrations.

Wavelet bases may be orthogonal, semi-orthogonal or simply bi-orthogonal. As we shall see later in more detail, over these three types, orthogonal wavelet is the only one which gives direct access to best approximation by discarding wavelet coefficients. Unfortunately, there is no orthogonal triangular Haar bases on the sphere. To overcome this lack, the concept of nearly orthogonality was introduced in [4]. A spherical wavelet basis is said to be nearly orthogonal if it becomes orthogonal when the subdivision depth increases (i.e. when the spherical triangles become planar). Two wavelet bases that are nearly orthogonal were given in [4].

*LMC-CNRS, BP.53, F-38041 Grenoble Cedex 9, France.

In this paper, we extend the results of [4] in the following directions. First, we give two one-parameter families of spherical Haar wavelet bases that are nearly orthogonal and simpler than in [4]. Then we introduce a measure of orthogonality. This measure vanishes for orthogonal bases, and converges to zero for nearly orthogonal bases, as the subdivision depth increases. Eventually, we show that there exist an optimal parameter value for our new wavelet families, for which the measure of orthogonality is minimal.

This paper is structured as follows. In section 2, we give the basics on piecewise constant triangular Haar wavelets. Section 3 is a review of the concept of orthogonality, semi-orthogonality, and nearly orthogonality in the context of triangular Haar wavelets. In section 4, the two new nearly orthogonal one-parameter families of wavelets are introduced. Section 5 is dedicated to the measure of orthogonality and to the optimization of this measure over the new families of wavelets. Eventually, section 6 illustrates our results on an earth topography data set.

2 Piecewise constant triangular wavelets

Piecewise constant triangular wavelets are defined by their values on the four subtriangles dividing their support. For each triangle in the nested grid, there exist three triangular Haar wavelets whose support matches exactly with that triangle. The global decomposition/reconstruction process of a data set in this wavelet basis consists in the recursive application of a local decomposition/reconstruction process.

Local decomposition/reconstruction

Let T^k be a triangle at the subdivision depth k ($k = 0$ for the base mesh). Let $T_0^{k+1}, T_1^{k+1}, T_2^{k+1}, T_3^{k+1}$ be the four sub-triangles of T^k . Let Ψ_1^k, Ψ_2^k and Ψ_3^k denote the three wavelet functions whose support matches T^k , and r_{ij}^k denote the value of Ψ_j^k on the sub-triangle T_i^{k+1} . Eventually, let Φ^k denote the constant function whose value is 1 on T^k . Fig. 2 illustrates these notations, and section 3 includes a practical numerical example of wavelet functions Ψ_1^k, Ψ_2^k and Ψ_3^k . The fundamental property of triangular Haar wavelets is that every piecewise constant function on the four sub-triangles ($T_i^{k+1}, i = 0, 1, 2, 3$) can be written as a linear combination of the constant function and the three wavelets:

$$\begin{array}{c} x_3^{k+1} \\ x_0^{k+1} \\ x_1^{k+1} \\ x_2^{k+1} \end{array} = x^k \Phi^k + y_1^k \Psi_1^k + y_2^k \Psi_2^k + y_3^k \Psi_3^k.$$

The relation that gives the values x_i^{k+1} of the left-hand side function from the wavelet coefficients y_i^k is referred to as local reconstruction:

$$\begin{pmatrix} x_0^{k+1} \\ x_1^{k+1} \\ x_2^{k+1} \\ x_3^{k+1} \end{pmatrix} = \begin{pmatrix} 1 & r_{01}^k & r_{02}^k & r_{03}^k \\ 1 & r_{11}^k & r_{12}^k & r_{13}^k \\ 1 & r_{21}^k & r_{22}^k & r_{23}^k \\ 1 & r_{31}^k & r_{32}^k & r_{33}^k \end{pmatrix} \begin{pmatrix} x^k \\ y_1^k \\ y_2^k \\ y_3^k \end{pmatrix} \quad (1)$$

Let R denote the so-called reconstruction matrix in (1). The inverse process of (1) is referred to as local decomposition:

$$\begin{pmatrix} x^k \\ y_1^k \\ y_2^k \\ y_3^k \end{pmatrix} = \begin{pmatrix} R^{-1} \end{pmatrix} \begin{pmatrix} x_0^{k+1} \\ x_1^{k+1} \\ x_2^{k+1} \\ x_3^{k+1} \end{pmatrix} \quad (2)$$

Global decomposition / reconstruction

Given the values (x_i^K) of an input data set at the maximal depth level K , the decomposition in the wavelet basis can be described by the following pseudo-code:

```
for k = K - 1 to 0
  for all triangles  $T^k$  at level k
    perform local decomposition (2)
    store  $(x^k, y_1^k, y_2^k, y_3^k)$  instead of  $(x_0^{k+1}, x_1^{k+1}, x_2^{k+1}, x_3^{k+1})$ 
```

This decomposition process outputs one value on each triangle of the base mesh, and a set of three wavelet coefficients for each triangle in the nested grid. The global reconstruction is the straightforward inverse process:

```
for k = 0 to K - 1
  for all triangles  $T^k$  at level k
    perform local reconstruction (1)
    store  $(x_0^{k+1}, x_1^{k+1}, x_2^{k+1}, x_3^{k+1})$  instead of  $(x^k, y_1^k, y_2^k, y_3^k)$ 
```

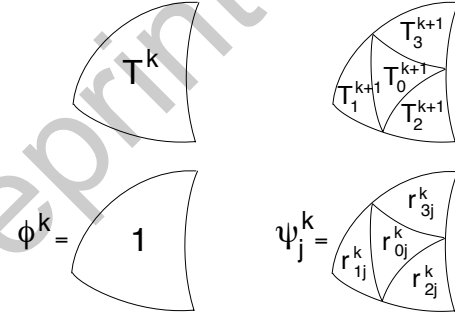


Figure 2: basis functions at level k

3 Orthogonality, semi-orthogonality and nearly orthogonality

We will review the concepts of orthogonality, semi-orthogonality and nearly orthogonality in the context of spherical triangular Haar wavelets, although the first two of them are much more general.

Orthogonality / semi-orthogonality

Here we use the notations of section 2. A function at level $k + 1$ is decomposed in the wavelet basis:

$$\begin{array}{c} x_3^{k+1} \\ x_0^{k+1} \\ x_1^{k+1} \\ x_2^{k+1} \end{array} = x^k \Phi^k + y_1^k \Psi_1^k + y_2^k \Psi_2^k + y_3^k \Psi_3^k.$$

The wavelet basis is defined as semi-orthogonal, if the inner product of the wavelets with the constant function vanishes:

$$\int \Psi_1^k \Phi^k = \int \Psi_2^k \Phi^k = \int \Psi_3^k \Phi^k = 0.$$

The wavelet basis is defined as orthogonal, if in addition to the semi-orthogonality condition, any two distinct wavelet functions have a vanishing inner product:

$$\int \Psi_1^k \Psi_2^k = \int \Psi_1^k \Psi_3^k = \int \Psi_2^k \Psi_3^k = 0.$$

We can illustrate the weakness of semi-orthogonal bases on a simple example.

Assume the triangles are planar, and the areas of the four sub-triangles equal identically one. In this case, the semi-orthogonal basis introduced in [5] is the following:

$$\Phi = \begin{array}{|c|} \hline 1 \\ \hline \end{array} \quad \Psi_1 = \begin{array}{|c|} \hline 1 \\ \hline -3 \quad 1 \quad 1 \\ \hline \end{array} \quad \Psi_2 = \begin{array}{|c|} \hline 1 \\ \hline 1 \quad 1 \quad -3 \\ \hline \end{array} \quad \Psi_3 = \begin{array}{|c|} \hline -3 \\ \hline 1 \quad 1 \quad 1 \\ \hline \end{array}$$

We wish to represent the following function F using this basis:

$$F = \begin{array}{|c|} \hline 0 \\ \hline 1 \quad 3 \quad 0 \\ \hline \end{array}$$

The exact decomposition of F in the wavelet basis is:

$$F = 1 \cdot \Phi + \frac{1}{2} \Psi_1 + \frac{3}{4} \Psi_2 + \frac{3}{4} \Psi_3$$

The approximation of F after discarding the lowest wavelet coefficient (compression gain: 25%) is:

$$1 \cdot \Phi + \frac{3}{4} \Psi_2 + \frac{3}{4} \Psi_3 = \begin{array}{|c|} \hline -1/2 \\ \hline 5/2 \quad 5/2 \quad -1/2 \\ \hline \end{array}$$

The L^2 error for this approximation is $\sqrt{3}$.

The best approximation of F with the same three basis functions Φ, Ψ_2, Ψ_3 is:

$$1 \cdot \Phi + \frac{1}{2} \Psi_2 + \frac{1}{2} \Psi_3 = \begin{array}{|c|} \hline 0 \\ \hline 2 \quad 2 \quad 0 \\ \hline \end{array}$$

In this case, the L^2 error is reduced to $\sqrt{2}$. Therefore, approximation by discarding the lowest wavelet coefficient, results in an L^2 error that is 22% larger than the best L^2 error with the same wavelet functions.

This illustrates one advantage of orthogonal bases over semi-orthogonal bases: the best L^2 error obtained by keeping a certain subset of the wavelet functions is always obtained for the corresponding wavelet coefficients.

Nearly orthogonality

The concept of nearly orthogonality for spherical wavelets was introduced in [4]. As the subdivision depth increases, the spherical triangles become planar, and the areas of the four sub-triangles become uniform. On the other hand, the three wavelet functions depend on the areas of these sub-triangles. A wavelet basis is defined as nearly orthogonal, if it is orthogonal in the limit case, i.e. when the four sub-triangle areas are equal.

4 Families of nearly orthogonal spherical Haar wavelets

In this section, we introduce new spherical Haar wavelets, that are nearly orthogonal, and that depend on one free parameter. In addition to the previous notations given in section 2, we denote $\alpha_0^k, \alpha_1^k, \alpha_2^k, \alpha_3^k$ the areas of the four sub-triangles $T_0^k, T_1^k, T_2^k, T_3^k$.

Previous spherical triangular Haar bases

In order to simplify the notations, we will always give the unnormalized reconstruction matrices: to find the effective, L^2 -normalized reconstruction matrices, each column has to be divided by the square rooted sum of the squared coefficients weighted by the areas; and each line i has to be multiplied by $\sqrt{\alpha_i}$. In other words, if $\tilde{R} = (\tilde{r}_{ij})$ is the unnormalized reconstruction matrix, the effective reconstruction matrix $R = (r_{ij})$ is given by:

$$r_{ij} = \tilde{r}_{ij} \cdot \frac{\sqrt{\alpha_i}}{\sqrt{\tilde{r}_{0j}\alpha_0 + \tilde{r}_{1j}\alpha_1 + \tilde{r}_{2j}\alpha_2 + \tilde{r}_{3j}\alpha_3}} \quad i, j = 0, 1, 2, 3.$$

In [5], the following unnormalized reconstruction matrix was introduced:

$$\begin{pmatrix} 1 & -\alpha_1 & -\alpha_2 & -\alpha_3 \\ 1 & \alpha_0 + \alpha_2 + \alpha_3 & -\alpha_2 & -\alpha_3 \\ 1 & -\alpha_1 & -\alpha_0 + \alpha_1 + \alpha_3 & -\alpha_3 \\ 1 & -\alpha_1 & -\alpha_2 & \alpha_0 + \alpha_1 + \alpha_2 \end{pmatrix} \quad (3)$$

This corresponds to a semi-orthogonal basis, since $\int \Psi_1 = \int \Psi_2 = \int \Psi_3 = 0$ with this matrix.

This basis is not nearly orthogonal, since in the limit case of uniform areas, i.e. when $\alpha = \alpha_0 = \alpha_1 = \alpha_2 = \alpha_3$, we have the following inner products:

$$\int \Psi_1 \Psi_2 = \int \Psi_1 \Psi_3 = \int \Psi_2 \Psi_3 = -4\alpha^3 \neq 0.$$

In [4], the following unnormalized reconstruction matrices were proposed:

$$\begin{pmatrix} 1 & \Delta - \alpha_0^2 - \alpha_0\alpha_1 & \Delta - \alpha_0^2 - \alpha_0\alpha_2 & \Delta - \alpha_0^2 - \alpha_0\alpha_3 \\ 1 & \Delta - \alpha_1^2 - \alpha_0\alpha_1 & -\alpha_0\alpha_1 - \alpha_1\alpha_2 & -\alpha_0\alpha_1 - \alpha_1\alpha_3 \\ 1 & -\alpha_0\alpha_2 - \alpha_1\alpha_2 & \Delta - \alpha_2^2 - \alpha_0\alpha_2 & -\alpha_0\alpha_2 - \alpha_2\alpha_3 \\ 1 & -\alpha_0\alpha_3 - \alpha_1\alpha_3 & -\alpha_0\alpha_3 - \alpha_2\alpha_3 & \Delta - \alpha_3^2 - \alpha_0\alpha_3 \end{pmatrix} \quad (4)$$

and

$$\begin{pmatrix} 1 & \Delta - \alpha_0^2 + 3\alpha_0\alpha_1 & \Delta - \alpha_0^2 + 3\alpha_0\alpha_2 & \Delta - \alpha_0^2 + 3\alpha_0\alpha_3 \\ 1 & -3(\Delta - \alpha_1^2) - \alpha_0\alpha_1 & -\alpha_0\alpha_1 + 3\alpha_1\alpha_2 & -\alpha_0\alpha_1 + 3\alpha_1\alpha_3 \\ 1 & -\alpha_0\alpha_2 + 3\alpha_1\alpha_2 & -3(\Delta - \alpha_2^2) - \alpha_0\alpha_2 & -\alpha_0\alpha_2 + 3\alpha_2\alpha_3 \\ 1 & -\alpha_0\alpha_3 + 3\alpha_1\alpha_3 & -\alpha_0\alpha_3 + 3\alpha_2\alpha_3 & -3(\Delta - \alpha_3^2) + 3\alpha_0\alpha_3 \end{pmatrix} \quad (5)$$

where $\Delta = \alpha_0^2 + \alpha_1^2 + \alpha_2^2 + \alpha_3^2$. Both of these matrices were proved to be semi-orthogonal and also nearly orthogonal in [4].

New families of nearly orthogonal Haar bases

A quick look at previously introduced reconstruction matrices (3), (4), (5) shows the 4×3 sub-matrices containing the wavelet function values are polynomials in the sub-triangle areas $\alpha_0, \alpha_1, \alpha_2, \alpha_3$. The degree is 2 for the matrices (4) and (5) and 1 for the matrix (3).

Since we wanted to find both simple (i.e. with low degree polynomial coefficients), and nearly orthogonal matrices, we have started with a 4×3 sub-matrix containing arbitrary polynomials of degree 1 (linear functions) in $\alpha_0, \alpha_1, \alpha_2, \alpha_3$. Without any condition on the coefficients of these polynomials, the number of free parameters would be $4 \times 3 \times 4 = 48$.

A first condition that has to be fulfilled is symmetry. This property states that, when permuting the indices (1,2,3) in the right and left-hand side of the local decomposition/reconstruction relations

(1) and (2), the equality should be preserved. Imposing symmetry reduces the number of free parameters from 48 to 10.

The second condition is semi-orthogonality. This condition reduces further the number of free parameters to three, and we get the following unnormalized, semi-orthogonal families of reconstruction matrices:

$$\begin{pmatrix} 1 & a\alpha_1 + b\alpha_2 + b\alpha_3 & b\alpha_1 + a\alpha_2 + b\alpha_3 & b\alpha_1 + b\alpha_2 + a\alpha_3 \\ 1 & -a\alpha_0 + c\alpha_2 + c\alpha_3 & -b\alpha_0 - c\alpha_2 & -b\alpha_0 - c\alpha_3 \\ 1 & -b\alpha_0 - c\alpha_1 & -a\alpha_0 + c\alpha_1 + c\alpha_3 & -b\alpha_0 - c\alpha_3 \\ 1 & -b\alpha_0 - c\alpha_1 & -b\alpha_0 - c\alpha_2 & -a\alpha_0 + c\alpha_1 + c\alpha_2 \end{pmatrix} \quad (6)$$

Here a, b, c are the free parameters. As a special case of (6), the semi-orthogonal reconstruction matrix (3) of [5] is obtained for $a = -1, b = 0$ and $c = 1$.

The last condition to impose is nearly-orthogonality. In the limit case of uniform areas, i.e. $\alpha = \alpha_0 = \alpha_1 = \alpha_2 = \alpha_3$, the inner products of the wavelet functions yield:

$$\int \Psi_1 \Psi_2 = \int \Psi_1 \Psi_3 = \int \Psi_2 \Psi_3 = \alpha^3 (a^2 + 5b^2 - 3c^2 + 6ab + 2ac - 2bc)$$

These inner products vanish if and only if

$$\begin{cases} c = a + b \\ \text{or} \\ c = -\frac{a+5b}{3} \end{cases}$$

Thus, we have two new families of symmetric, semi-orthogonal and nearly orthogonal triangular wavelets:

$$\begin{pmatrix} 1, & a\alpha_1 + b\alpha_2 + b\alpha_3, & b\alpha_1 + a\alpha_2 + b\alpha_3, & b\alpha_1 + b\alpha_2 + a\alpha_3 \\ 1, & -a\alpha_0 + (a+b)(\alpha_2 + \alpha_3), & -b\alpha_0 - (a+b)\alpha_2, & -b\alpha_0 - (a+b)\alpha_3 \\ 1, & -b\alpha_0 - (a+b)\alpha_1, & -a\alpha_0 + (a+b)(\alpha_1 + \alpha_3), & -b\alpha_0 - (a+b)\alpha_3 \\ 1, & -b\alpha_0 - (a+b)\alpha_1, & -b\alpha_0 - (a+b)\alpha_2, & -a\alpha_0 + (a+b)(\alpha_1 + \alpha_2) \end{pmatrix} \quad (7)$$

$$\begin{pmatrix} 1, & a\alpha_1 + b\alpha_2 + b\alpha_3, & b\alpha_1 + a\alpha_2 + b\alpha_3, & b\alpha_1 + b\alpha_2 + a\alpha_3 \\ 1, & -a\alpha_0 - \left(\frac{a+5b}{3}\right)(\alpha_2 + \alpha_3), & -b\alpha_0 + \left(\frac{a+5b}{3}\right)\alpha_2, & -b\alpha_0 + \left(\frac{a+5b}{3}\right)\alpha_3 \\ 1, & -b\alpha_0 + \left(\frac{a+5b}{3}\right)\alpha_1, & -a\alpha_0 - \left(\frac{a+5b}{3}\right)(\alpha_1 + \alpha_3), & -b\alpha_0 + \left(\frac{a+5b}{3}\right)\alpha_3 \\ 1, & -b\alpha_0 + \left(\frac{a+5b}{3}\right)\alpha_1, & -b\alpha_0 + \left(\frac{a+5b}{3}\right)\alpha_2, & -a\alpha_0 - \left(\frac{a+5b}{3}\right)(\alpha_1 + \alpha_2) \end{pmatrix} \quad (8)$$

It should be kept in mind that (7) and (8) must be normalized, and this implies that there is really only one free parameter in (7) and (8). In fact, we can assume without restriction that $a = 1$ in the rest of this paper (more precisely, if $a \neq 1$, then replacing a by one, and b by $\frac{b}{a}$ gives the same matrix after normalization).

Thus (7) and (8) define two one parameter families of wavelet bases that are symmetric, semi-orthogonal, and orthogonal if $\alpha_0 = \alpha_1 = \alpha_2 = \alpha_3$.

5 Orthogonality measure and optimal Haar bases

In section 4, three previous wavelet bases were recalled, and two new families of wavelet bases were introduced. We now introduce a measure to distinguish all these wavelet bases and we show that, for the wavelet families (7) and (8), optimal values with respect to this measure can be calculated.

Since our main concern is on the orthogonality of the bases, the following measure was chosen:

$$M(K) = \frac{1}{n} \sum_{k=1}^K \sum_{T^k} \left| \int \Psi_1^k \Psi_2^k \right| + \left| \int \Psi_1^k \Psi_3^k \right| + \left| \int \Psi_2^k \Psi_3^k \right| \quad (9)$$

Here K is the finest subdivision level, n is the number of triangles at that level (n equals to the number of base faces times 4^K), k traverses all levels, and T^k traverses all triangles at the level k .

A straightforward property of the orthogonality measure (9) is that it vanishes if and only if all inner products also vanish, i.e. if the wavelet basis is orthogonal.

Another property of this measure is illustrated in Fig. 3. This figure shows the behaviour of the orthogonality measure (9) for the semi-orthogonal basis (3) introduced in [5], and for the new nearly orthogonal wavelets (7) with parameters $a = 1$ and $b = 0$. The measure (9) has been computed at increasing subdivision depths K , and for three base spherical triangulations (tetrahedron, octahedron, icosahedron). The behaviour of the measure (9) is the same for the three nested triangulations: for the semi-orthogonal basis (3) it increases up to a limit, and for the nearly orthogonal basis (7) with $a = 1$ and $b = 0$ it decreases and converges to zero. This is due to the fact that the inner products in (9) converge to a non-zero value for the semi-orthogonal basis (3) and to zero for all nearly orthogonal bases.

Thus we see that the orthogonality measure (9) allows to distinguish the semi-orthogonal and the nearly orthogonal bases.

It can also be observed that the measure decreases more quickly for the nested grid based on an icosahedron. This is because the triangles become more quickly uniform for this grid.

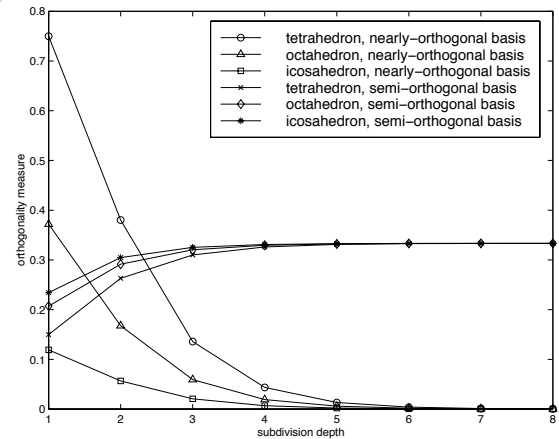


Figure 3: Orthogonality measure (9) for the semi-orthogonal basis (3) introduced in [5] and for the new nearly-orthogonal wavelet basis (7) with parameters $a = 1, b = 0$. The measure (9) is computed at increasing subdivision depths and for three different nested spherical triangulations.

In the rest of this section, we use the orthogonality measure (9) to find an optimal basis between the two new families of bases (7) and (8).

In order to do this, we have fixed a certain subdivision depth K , and compute the orthogonality measure (9) for different values of

family (7)		
Base mesh	optimal parameter values	optimal orthogonality measure
tetrahedron	$a \equiv 1$ $b \equiv -1.707$	$2.28 \cdot 10^{-2}$
octahedron	$a \equiv 1$ $b \equiv -1.592$	$6.44 \cdot 10^{-3}$
icosahedron	$a \equiv 1$ $b \equiv -1.535$	$1.14 \cdot 10^{-3}$

family (8)		
Base mesh	optimal parameter values	optimal orthogonality measure
tetrahedron	$a \equiv 1$ $b \equiv -0.051$	$2.72 \cdot 10^{-3}$
octahedron	$a \equiv 1$ $b \equiv -0.061$	$8.99 \cdot 10^{-5}$
icosahedron	$a \equiv 1$ $b \equiv -0.067$	$1.62 \cdot 10^{-5}$

Table 1: These tables give the optimal parameter values for the two new families of wavelet bases (7) and (8), and the corresponding optimal orthogonality measure. The optimal parameter values have been computed for three different nested triangulations, at the subdivision depth 5, and up to a precision 10^{-3} .

the free parameters in the bases (7) and (8). Fig. 4a shows a plot of the results for the family (7), with parameters $a = 1$ and b increasing from -50 to 50, for the three different nested triangulations, and at the subdivision depth 3. This plot suggests that there exist optimal parameter values for which the orthogonality measure (9) is minimal. Fig. 4b shows a zoom for the parameter values $a = 1$, b increasing from -2 to -1. On this plot, the optimal parameter values for the family (7) are now clearly visible. The same behaviour is shown on figures 4c and 4d for the wavelet family (8).

Figure 4 shows also that the family (8) enables to reach a significantly smaller orthogonality measure. In table 1, the computed optimal values at the depth 5, up to a precision 10^{-3} , together with the corresponding orthogonality measure (9) are given.

6 Results

The new nearly orthogonal bases (7) and (8) with optimal values given in table 1 have been tested and compared against the previous semi-orthogonal basis (3). The tests were performed on three nested spherical triangulations (base mesh tetrahedron, octahedron and icosahedron), subdivided to the level 7. The original topographic data set, available from the National Oceanographic and Atmospheric Administration¹ is a 4320×2160 uniform grid of short values. This data set was mapped on the finest triangulation in order to find the input data values of the wavelet decomposition algorithm. The mapping was done by a simple trapezoid quadrature formula that computes the integral of the original data on the finest triangles. The data set was then decomposed and reconstructed with an increasing number of wavelet coefficients. For each test, the difference between the true L^2 error and the square rooted sum of the squared wavelet coefficients was computed. This measures the orthogonality of the wavelet basis with respect to the input data set in the following sense: it vanishes for orthogonal bases, and increases when the inner products of the wavelets modify the true L^2 error.

Table 2 gives the numerical results. It clearly shows that our new

¹at

ftp://ftp.ngdc.noaa.gov/Solid_Earth/Topography/tbase_5min/

# way. coeff.	comp. gain	basis (3)	basis (7)	basis (8)
500	99.2 %	1.11 %	0.32 %	0.036 %
2000	96.9 %	1.76 %	0.30 %	0.034 %
6000	90.8 %	1.47 %	0.30 %	0.033 %
10000	84.7 %	1.04 %	0.30 %	0.033 %

Base mesh: spherical tetrahedron

# way. coeff.	comp. gain	basis (3)	basis (7)	basis (8)
1000	99.2 %	1.27 %	0.05 %	0.0056 %
5000	96.2 %	1.36 %	0.05 %	0.0052 %
10000	92.4 %	0.78 %	0.05 %	0.0052 %
20000	84.7 %	0.58 %	0.05 %	0.0051 %

Base mesh: spherical octahedron

# way. coeff.	comp. gain	basis (3)	basis (7)	basis (8)
5000	98.5 %	2.44 %	0.0039 %	0.00058 %
10000	96.9 %	2.30 %	0.0040 %	0.00054 %
20000	94.0 %	1.90 %	0.0040 %	0.00052 %
40000	87.8 %	1.59 %	0.0040 %	0.00051 %

Base mesh: spherical icosahedron

Table 2: These tables give the relative difference between the true L^2 error and the square rooted sum of the squared wavelet coefficients used for the reconstruction of the topographic data set. This difference vanishes for orthogonal bases, and should be smaller as possible. The tables show, in particular for the spherical icosahedron base mesh, that the difference is infinitesimal for our optimal wavelet bases (7) and (8).

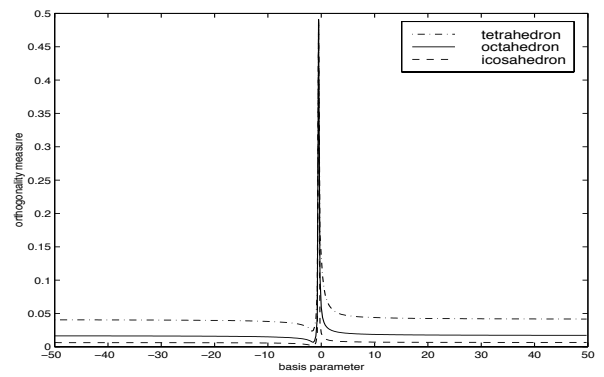
wavelet bases (7) and (8) with the optimal parameters given in table 1 greatly reduces the L^2 error due to the non-orthogonality of the basis functions.

The color plate shows some partial reconstructions obtained with the wavelet basis (8) and optimal parameter values, for the spherical icosahedron nested triangulation. The base mesh can be seen in red on each figure.

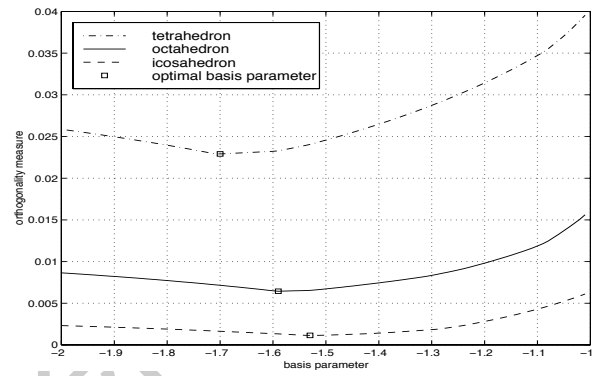
References

- [1] Georges-Pierre Bonneau. Multiresolution analysis on irregular surface meshes. *IEEE Transactions on Visualization and Computer Graphics*, 4(4):365–378, December 1998.
- [2] M. H. Gross, L. Lippert, R. Dittich, and S. Häring. Two methods for Wavelet-Based volume rendering. *Computers & Graphics*, 21(2):237–252, 1997.
- [3] Michael Lounsbery, Tony D. DeRose, and Joe Warren. Multiresolution analysis for surfaces of arbitrary topological type. *ACM Transactions on Graphics*, 16(1):34–73, January 1997.
- [4] Gregory M. Nielson, Il-Hong Jung, and Junwon Sung. Haar-wavelets over triangular domains with applications to multiresolution models for flow over a sphere. In *IEEE Visualization '97*, pages 143–150. IEEE, November 1997.
- [5] Peter Schröder and Wim Sweldens. Spherical wavelets: Efficiently representing functions on the sphere. In *SIGGRAPH 95 Conference Proceedings*, pages 161–172. ACM SIGGRAPH, August 1995.

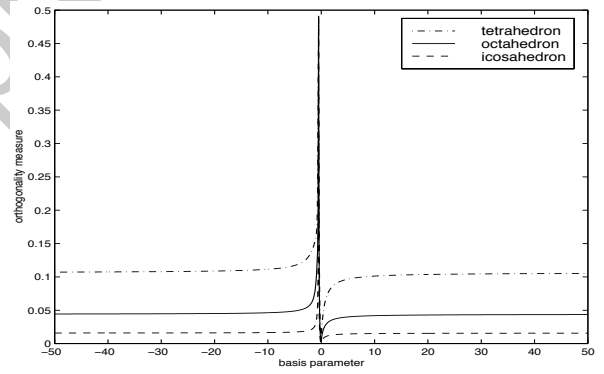
[6] Eric J. Sollnitz, Tony D. DeRose, and David H. Salesin. *Wavelets for Computer Graphics: Theory and Applications*. Morgan Kaufmann Publishers, 1996.



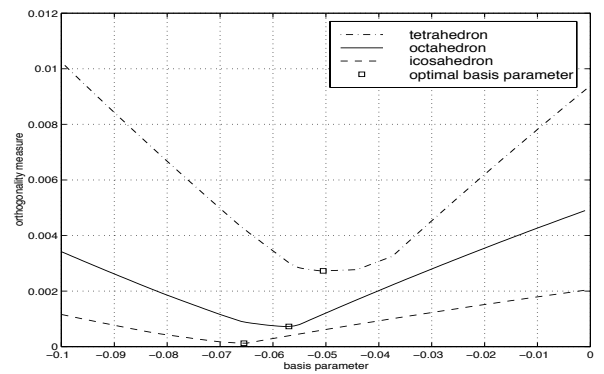
(a)



(b)



(c)



(d)

Figure 4: Orthogonality measure for the new wavelet bases (7) (figs (a) and (b)) and (8) (figs (c) and (d)), computed at the subdivision depth 3. The parameter a is fixed to 1, and the parameter b is chosen on the X-axis. These plots show the existence of optimal parameter values for which the orthogonality measure is minimal.